The mammary gland iodide transporter is expressed during lactation and in breast cancer

UYGAR H. TAZEBAY[1], IRENE L. WAPNIR[5], ORLIE LEVY[1,7], ORSOLYA DOHAN[1], LIONEL S. ZUCKIER[2], QING HUA ZHAO[2], HOU FU DENG[2], PETER S. AMENTA[6], SUSAN FINEBERG[4], RICHARD G. PESTELL[3] & NANCY CARRASCO[1]

[1]*Department of Molecular Pharmacology,* [2]*Department of Nuclear Medicine*
[3]*Department of Medicine and Developmental and Molecular Biology, Albert Einstein College of Medicine*
1300 Morris Park Avenue Bronx, New York 10461, USA
[4]*Department of Pathology, Montefiore Medical Center, Bronx, New York 10467, USA*
[5]*Department of Surgery,* [6]*Department of Pathology UMDNJ-Robert Wood Johnson Medical School*
New Brunswick, New Jersey 08903, USA [7]*Wyeth-Lederle Vaccines*
401 North Middletown Rd 180/216-17 Pearl River, New York 10965
U.H.T. and I.L.W. contributed equally to this study.
Correspondence should be addressed to N.C.; email: carrasco@aecom.yu.edu

The sodium/iodide symporter mediates active iodide transport in both healthy and cancerous thyroid tissue. By exploiting this activity, radioiodide has been used for decades with considerable success in the detection and treatment of thyroid cancer. Here we show that a specialized form of the sodium/iodide symporter in the mammary gland mediates active iodide transport in healthy lactating (but not in nonlactating) mammary gland and in mammary tumors. In addition to characterizing the hormonal regulation of the mammary gland sodium/iodide symporter, we demonstrate by scintigraphy that mammary adenocarcinomas in transgenic mice bearing *Ras* or *Neu* oncogenes actively accumulate iodide by this symporter *in vivo.* Moreover, more than 80% of the human breast cancer samples we analyzed by immunohistochemistry expressed the symporter, compared with none of the normal (nonlactating) samples from reductive mammoplasties. These results indicate that the mammary gland sodium/iodide symporter may be an essential breast cancer marker and that radioiodide should be studied as a possible option in the diagnosis and treatment of breast cancer.

Iodide, an essential constituent of the thyroid hormones T_3 and T_4, is accumulated in the thyroid by means of a highly specialized active iodide transport mechanism[1] catalyzed by the sodium/iodide symporter (Na^+/I^- symporter, called NIS here), an essential glycoprotein located in the basolateral plasma membrane of the thyroid follicular cells[2]. NIS-catalyzed iodide accumulation is a sodium-dependent active transport driven by the sodium gradient maintained by the sodium/potassium ATPase. NIS is predicted to contain 13 transmembrane segments with extracellular N and intracellular C termini[3,4] and a 2:1 sodium:iodide stoichiometry[5].

Besides the thyroid, active iodide transport occurs in the lactating mammary gland, salivary glands and gastric mucosa[1]. Iodide concentrated in lactating mammary gland and secreted into milk is used by the nursing newborn for the biosynthesis of thyroid hormones[6,7], which are essential for proper development of the nervous system, skeletal muscle and lungs[8,9]. The mammary gland iodide transporter was the essential link in the chain of events that led to a higher thyroid cancer incidence in the aftermath of the Chernobyl power plant accident. ^{131}I in radioactive fallout was accumulated by cattle in milk, and children who ingested ^{131}I-contaminated milk subsequently concentrated ^{131}I in their thyroids through the thyroid NIS, exposing the gland to tumorigenic doses of radiation[10–12].

The degree and pattern of iodide accumulation in the thyroid are central factors in the differential diagnosis of thyroid nodules. Moreover, radioactive iodide is used in the postoperative management of differentiated thyroid carcinoma, ablating remnant thyroid tissue and metastases[9,13]. A comparable approach might be feasible in breast cancer if the mammary gland iodide transporter were expressed in mammary tumors. Here we report the identification of the protein that transports iodide in mammary tissue, called the mammary gland NIS (mgNIS); the characterization of several of its molecular and physiological

Table 1 mgNIS expression in human breast cancer

Breast histology	Number of samples	mgNIS-positive	Estrogen-receptor-positive
Normal breast (reductive mammoplasty)	8	0 (0%)	ND
Invasive carcinomas	23	20 (87%)	56%
Ductal carcinoma *in situ*	6	5 (83%)	ND
Noncancerous in the vicinity of tumor	13	3 (23%)	ND
Gestational tissues	3	3 (100%)	ND

ND, not determined.

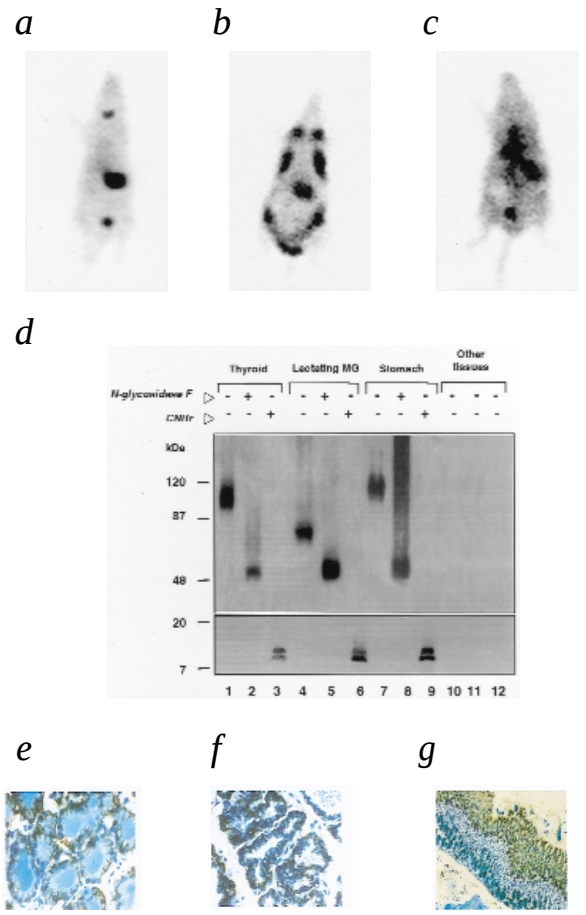

properties; the functional expression of mgNIS in experimental mammary adenocarcinomas in transgenic mice; and the high incidence (80%) of mgNIS expression in human breast cancer. Alternative strategies for the detection of micrometastatic breast disease and for more-effective and targeted systemic therapies are needed to improve survival in breast cancer, the leading cause of cancer deaths in women between the ages of 20 and 59 (ref. 14).

Fig. 1 TPT accumulation and NIS expression in rat stomach and lactating mammary gland. ***a*** and ***b***, *In vivo* scintigraphic imaging (ventral projection) of TPT-injected nubile (*a*) and lactating (*b*) rats. ***c***, Static imaging to ascertain perchlorate inhibition of TPT uptake. ***d***, Immunoblot analysis with NIS-specific antibody, with and without peptidyl *N*-glycosidase F digestion. Tissues: Lanes 1–9, above blot; lanes 3, 6 and 9, membrane fractions treated with cyanogen bromide (CNBr); lane 10, nonlactating mammary gland; lane 11, muscle; lane 12, lung. Left margin, molecular sizes. ***e***, ***f*** and ***g***, Immunohistochemical analysis of rat thyroid (*e*), lactating mammary gland (*f*) and stomach tissues (*g*), using the NIS-specific antibody used in *d* Original magnification, X200.

In vivo analysis of iodide accumulation in rat mammary tissue

To characterize the active accumulation of iodide in milk, we intraperitoneally injected lactating rats with ^{125}I and assessed the time course of ^{125}I transport in milk. The radioisotope was concentrated more than 6,000% in milk compared with its level in blood, with saturation occurring at about 2 hours (data not shown). ^{125}I was also concentrated in lactating mammary gland, but not in skeletal muscle from the same rat or in mammary gland from a nonlactating rat. To assess tissue distribution of iodide *in vivo*, rats received ^{131}I or technetium–pertechnetate (TPT) for scintigraphic imaging. TPT, a γ-emitting molecule actively concentrated in the thyroid by NIS, offers the practical advantage of a much shorter half-life (6 hours) than ^{131}I (half-life, 8 days; ref. 15). In nonlactating rats, we initially found the radioisotope mainly in the stomach, and later (more than 30 minutes) in the thyroid (Fig. 1*a*). In contrast, lactating rats rapidly concentrated TPT (within 5 minutes) in all pairs of mammary glands (Fig. 1*b*). Simultaneous injection of TPT with perchlorate, a potent inhibitor of active iodide transport[1], into a lactating rat effectively prevented TPT concentration in thyroid, stomach and lactating mammary gland (Fig. 1*c*), showing that ^{131}I/TPT accumulation in these tissues is specific and can be inhibited by perchlorate.

Identification of mammary gland NIS

A high-affinity, site-directed antibody against the C terminus of NIS reacts with a rat thyroid NIS polypeptide of about 100 kilodaltons (kDa) (ref. 3; Fig. 1*d*, lane 1). The same antibody identified a single broad polypeptide of about 75 kDa, designated the mgNIS, in mammary gland membranes of lactating rats (Fig. 1*d*,

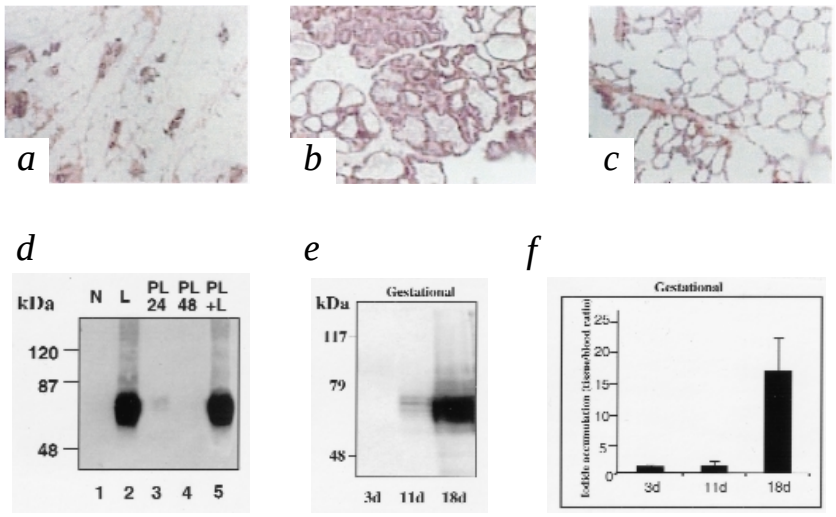

Fig. 2 mgNIS expression at different physiological stages in murine mammary gland. ***a***–***c***, Hematoxylin and eosin staining of nubile (*a*), lactating (*b*) and previously lactating rat (*c*) mammary glands. Original magnification, X30. ***d***, Immunoblot analysis of mgNIS expression in mammary glands at different physiological stages: nubile rats (lane 1); lactating dams (lane 2); and lactating dams after litter-weaning for 24 h (lane 3), 48 h (lane 4) or 48 h, followed by re-establishment of suckling for 24 h (lane 5). ***e***, Immunoblot analysis of mgNIS expression in membrane fractions of mammary gland tissue from mice at the third (3d), eleventh (11d) and eighteenth (18d) days of gestation. Left margins (*d* and *e*), molecular sizes. ***f***, Radioiodide accumulation in mammary glands from mice at the third (3d), eleventh (11d) and eighteenth (18d) days of gestation. Data were standardized to the weight of removed mammary gland from each mouse and are expressed as the ratio of radioiodide in mammary gland tissue to that in blood.

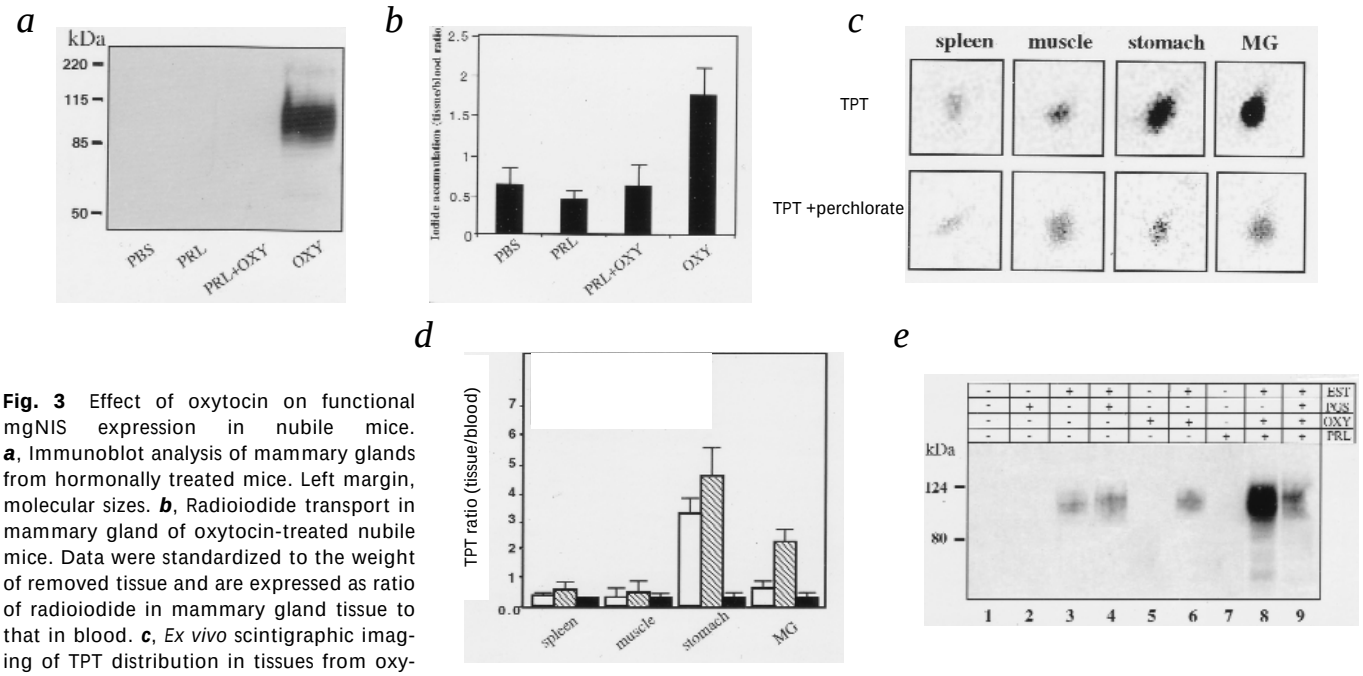

Fig. 3 Effect of oxytocin on functional mgNIS expression in nubile mice. ***a***, Immunoblot analysis of mammary glands from hormonally treated mice. Left margin, molecular sizes. ***b***, Radioiodide transport in mammary gland of oxytocin-treated nubile mice. Data were standardized to the weight of removed tissue and are expressed as ratio of radioiodide in mammary gland tissue to that in blood. ***c***, *Ex vivo* scintigraphic imaging of TPT distribution in tissues from oxytocin-treated nubile mice. ***d***, Quantification of TPT accumulation in various organs from oxytocin- or PBS-treated mice. Scintigraphic images in *c* were used to quantify TPT accumulation in spleen, skeletal muscle, stomach or mammary glands. Total counts were normalized by the weight of each organ (in counts per minute/mg tissue) and standardized by dividing by the ratio of count to weight for each mouse's blood. TPT accumulation in the organs from PBS–treated mice (□), oxytocin–treated mice (▨), or oxytocin– treated mice after injection of TPT plus perchlorate (■), presented as ratio of tissue to blood. ***e***, Immunoblot analysis of mammary glands from ovariectomized nubile mice treated for 3 consecutive days with hormones: PBS, lane 1; progesterone, lane 2; 17-β-estradiol, lane 3; 17-β-estradiol and progesterone, lane 4; oxytocin, lane 5; oxytocin and 17-β-estradiol, lane 6; prolactin, lane 7; oxytocin, prolactin and 17-β-estradiol, lane 8; progesterone together with oxytocin, prolactin and 17-β-estradiol, lane 9. Left margin, molecular sizes. PRL, prolactin; OXY, oxytocin; MG, mammary gland; PGS, progesterone; EST, 17-β-estradiol.

lane 4). In contrast, immunoreactivity was absent in nonlactating mammary gland (Fig. 1*d*, lane 10) and in membranes from muscle and lung (Fig. 1*d*, lanes 11 and 12). Immunoreactivity against both the approximately 75- and 100-kDa polypeptides was competitively blocked by addition of the synthetic eliciting peptide that contained the last 16 amino acids of NIS (data not shown). We treated membrane fractions from thyroid and lactating mammary gland with peptidyl N-glycosidase F, an enzyme that removes N-linked carbohydrates. In these conditions, NIS-specific antibody recognized a polypeptide of about 50 kDa in thyroid and lactating mammary gland (Fig. 1*d*, lanes 2 and 5, respectively), with electrophoretic mobility identical to that of nonglycosylated NIS in FRTL-5 cells (a highly functional thyroid cell line) and to that of NIS expressed in *Escherichia coli*[3]. Therefore, the immunoreactive polypeptides of about 75 kDa and 50 kDa detected in lactating mammary gland are glycosylated and nonglycosylated forms of mgNIS, respectively.

Accumulation of iodide in the stomach (Fig. 1*a*) is catalyzed by a gastric form of NIS. A gastric protein of about 110 kDa detected by the NIS-specific antibody (Fig. 1*d*, lane 7) was converted to the band of about 50 kDa after deglycosylation (Fig. 1*d*, lane 8). Methionine-specific cleavage of thyroid NIS, mammary gland NIS and gastric NIS using cyanogen bromide indicates that NIS is the same protein in each of these three tissues (Fig. 1*d*, lanes 3, 6 and 9). These results are consistent with the finding that the cDNAs encoding the human thyroid and mammary NIS proteins are identical[16]. We undertook immunohistochemical analysis using NIS-specific antibody on formalin-fixed, paraffin-embedded tissue sections derived from rat thyroid, mammary gland and stomach. Distinct basolateral plasma membrane reactivity indicative of NIS localization was evident in the thyroid follicular cells (Fig. 1*e*), lactating mammary gland epithelial cells (Fig. 1*f*), and gastric mucosa cells, specifically superficial luminal and neck cells (Fig. 1*g*).

Expression of mgNIS in various physiological stages

During gestation and lactation, the fatty stroma characteristic of the nubile rat mammary gland (Fig. 2*a*) is replaced by alveolar–ductal structures containing luminal secretions and epithelial cells with intracellular milk fat globules (Fig. 2*b*). Weaning promotes rapid involutional changes such as alveolar dilatation and flattening of the epithelium (Fig. 2*c*). We did immunoblot analysis on membrane fractions from mammary gland tissue from nubile, lactating and previously lactating rats (dams separated from their litters). mgNIS was absent in nubile mammary gland (Fig. 2*d*, lane 1), but present in lactating mammary gland (Fig. 2*d*, lane 2). At 24 hours after mice were weaned, mgNIS expression was substantially decreased in previously lactating mammary gland (Fig. 2*d*, lane 3), and by 48 hours, mgNIS was not detectable (Fig. 2*d*, lane 4). mgNIS expression was increased again after re-initiation of suckling (Fig. 2*d*, lane 5).

We investigated whether expression of mgNIS started in response to suckling or during gestation (Fig. 2*e*). Expression of an mgNIS protein of about 75 kDa was barely detectable at mid-gestation (day 11; Fig. 2*e*), whereas towards the end of gestation, there were higher levels of mgNIS expression and a substantial increase in ^{125}I transport (day 18; Fig. 2*e* and *f*). These data indicate that induction of mgNIS expression precedes suckling (Fig.

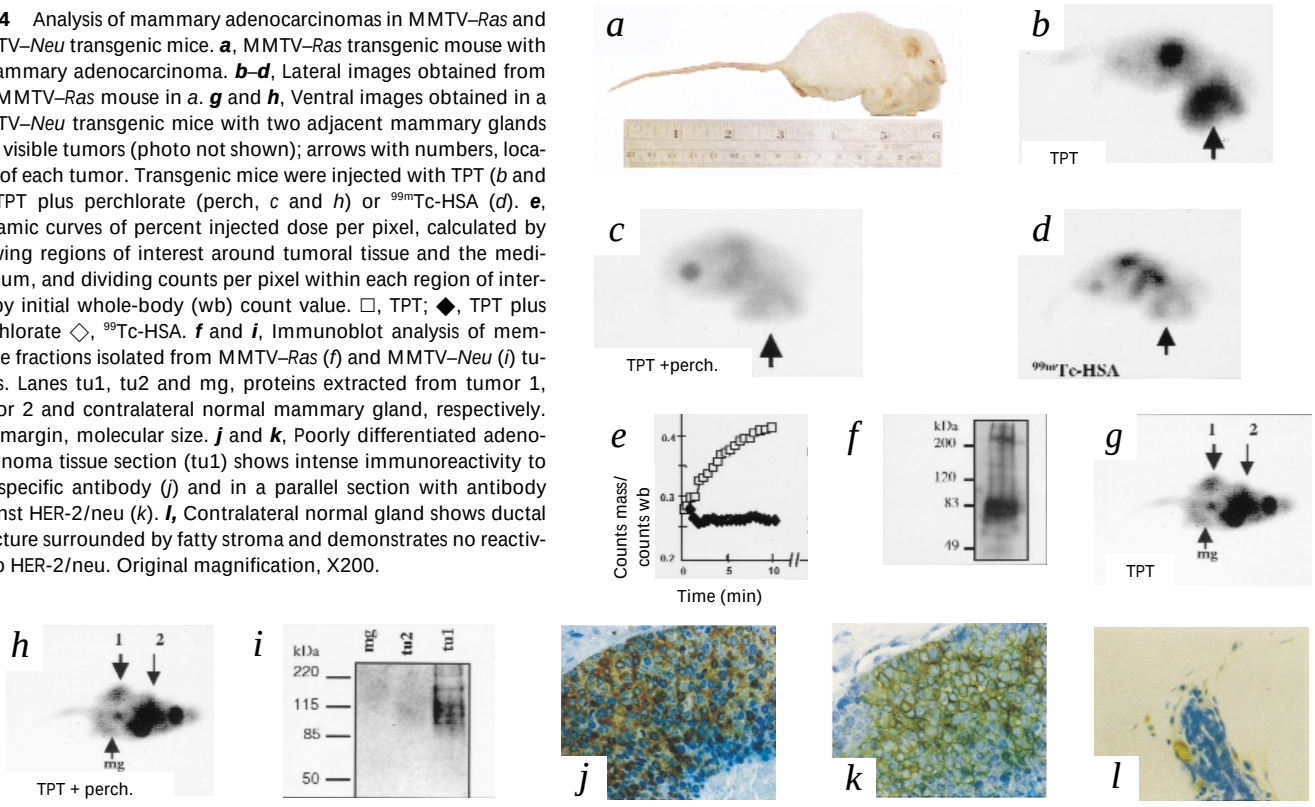

Fig. 4 Analysis of mammary adenocarcinomas in MMTV–*Ras* and MMTV–*Neu* transgenic mice. ***a***, MMTV–*Ras* transgenic mouse with a mammary adenocarcinoma. ***b–d***, Lateral images obtained from the MMTV–*Ras* mouse in *a*. ***g*** and ***h***, Ventral images obtained in a MMTV–*Neu* transgenic mice with two adjacent mammary glands with visible tumors (photo not shown); arrows with numbers, location of each tumor. Transgenic mice were injected with TPT (*b* and *g*), TPT plus perchlorate (perch, *c* and *h*) or ^{99m}Tc-HSA (*d*). ***e***, Dynamic curves of percent injected dose per pixel, calculated by drawing regions of interest around tumoral tissue and the mediastinum, and dividing counts per pixel within each region of interest by initial whole-body (wb) count value. □, TPT; ◆, TPT plus perchlorate ◇, ^{99}Tc-HSA. ***f*** and ***i***, Immunoblot analysis of membrane fractions isolated from MMTV–*Ras* (*f*) and MMTV–*Neu* (*i*) tumors. Lanes tu1, tu2 and mg, proteins extracted from tumor 1, tumor 2 and contralateral normal mammary gland, respectively. Left margin, molecular size. ***j*** and ***k***, Poorly differentiated adenocarcinoma tissue section (tu1) shows intense immunoreactivity to NIS-specific antibody (*j*) and in a parallel section with antibody against HER-2/neu (*k*). ***l,*** Contralateral normal gland shows ductal structure surrounded by fatty stroma and demonstrates no reactivity to HER-2/neu. Original magnification, X200.

2*e*), and that suckling is essential for increased expression of mgNIS after delivery (Fig. 2*d*).

Effects of hormones on mgNIS expression in intact mice

Both prolactin and oxytocin are released simultaneously in response to suckling[17,18]. However, only oxytocin alone, but not in combination with prolactin, induced mgNIS expression (Fig. 3*a*, lane OXY), leading to ^{125}I transport in mammary gland tissue (Fig. 3*b*). We administered a single dose of TPT with or without perchlorate to oxytocin- or sham-treated (PBS) nubile mice. Then, 30 minutes later, we surgically removed internal organs, as intense signal from the stomach during imaging interfered with that from the rudimentary mammary glands. We measured (Fig. 3*c*) and quantified (Fig. 3*d)* TPT accumulation in individual organs with a 'pinhole gamma camera'. As expected, accumulation of TPT in the stomachs of both oxytocin- and sham-treated mice was substantially greater than that in the spleens or limb skeletal muscles (Figs. 3*c* and *d*). In contrast, perchlorate-inhibitable TPT accumulation in mammary glands was substantially greater in oxytocin-treated mice than in sham-treated mice (Fig. 3*d*). The ability of oxytocin to induce functional mgNIS expression in the relatively undeveloped and undifferentiated mammary gland of nubile mice indicates that mgNIS synthesis can occur independently of gestation- and lactation-related changes. The antagonistic effect of prolactin on oxytocin action was unexpected, because mgNIS is upregulated in response to suckling, which stimulates the release of both hormones[17,18].

Effects of hormones on mgNIS expression in ovariectomized mice

We administered 17-β-estradiol, progesterone, oxytocin and prolactin, both individually and in different combinations, to nubile ovariectomized adult mice and assessed mgNIS expression in mammary tissue (Fig. 3*e*). Administration of oxytocin alone to ovariectomized mice did not cause an increase in mgNIS expression (Fig. 3*e*, lane 5), in contrast to the effect of oxytocin in intact mice (Fig. 3*a*). Of all the hormones tested individually, only 17-β-estradiol led to a clearly discernible increase in mgNIS expression (Fig. 3*e*, lane 3). Combined administration of 17-β-estradiol and oxytocin resulted in slightly higher mgNIS expression (Fig. 3*e*, lane 6) than did 17-β-estradiol alone (Fig. 3*e*, lane 3), indicating that the upregulating effect of oxytocin on mgNIS expression may require estrogen.

The greatest increase in mgNIS expression occurred after administration of 17-β-estradiol, oxytocin and prolactin together (Fig. 3*e*, lane 8), indicating that prolactin does not antagonize the upregulating effect of oxytocin on mgNIS expression; in fact, prolactin actually enhances this effect when estrogen levels are high. When progesterone was added to the 17-β-estradiol–oxytocin–prolactin combination, mgNIS expression was substantially decreased (Fig. 3*e*, lane 9). Conversely, a comparison of mgNIS expression in mice treated with estrogen or estrogen plus progesterone showed that progesterone did not interfere with 17-β-estradiol enhancement of mgNIS expression (Fig. 3*e*, lanes 3 and 4). In conclusion, the combination of estrogen, prolactin and oxytocin (in the absence of progesterone) led to the highest levels of mgNIS expression in ovariectomized mice. This combination of hormones closely resembles the relative hormonal levels in mice and rats during lactation[19,20].

Fucntional expression of mgNIS in mice mammary tumors

Physiologically, mammary gland epithelial cells express mgNIS only during late gestation and lactation, after the culmination of intense glandular proliferation and differentiation. Therefore, it

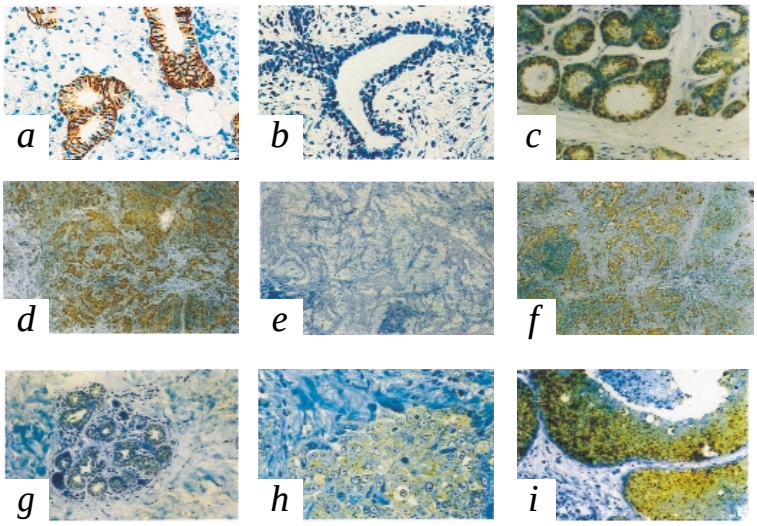

Fig. 5 NIS expression in human salivary gland and breast tissues. ***a***, Paraffin section of salivary gland treated with polyclonal Ct-2 antibody. ***b***, Normal breast tissue section without staining when treated with polyclonal Ct-2 antibody. ***c***, Gestational breast tissue with characteristic adenomatous–lactational changes occurring in the latter half of pregnancy demonstrates mgNIS expression in epithelial cells. ***d–f***, Invasive ductal carcinoma of the breast. *d* mgNIS expression detected with polyclonal Ct-2 antibody. *e*, Competitive inhibition of immunoreactivity with corresponding peptide. *f*, Parallel section treated with monoclonal antibody against NIS shows identical distribution of immunoreactivity to that in *d*. ***g***, Normal ductal–lobular units in the vicinity of breast cancer in *d–f*, assessed with monoclonal antibody against NIS. ***h***, Higher magnification of another invasive ductal carcinoma, showing focal areas of immunoreactivity with a very distinct intracellular staining pattern. ***i***, Ductal carcinoma *in situ* features intraductal comedonecrosis and intense immunoreactivity (more than 95%) of malignant cells with monoclonal antibody against NIS. Original magnifications, X100 (*a* and *b*), X80 (*c*), X16 (*d–f*), X40 (*g*), X160 (*h*) and X66 (*i*).

seems plausible that mgNIS could be expressed in cancer, as it also involves a proliferative process, albeit abnormal. We assessed functional expression of mgNIS in mammary tumors of two female transgenic mice, one with an activated *Ras* oncogene, and the other overexpressing the *Neu* oncogene (Genome DataBase designations, *c-Ha-ras* and *c-erbB-2*, respectively). Both genes were under the transcriptional control of the mouse mammary tumor virus (MMTV) promoter/enhancer[21,22]. The *Ras* oncogene encodes a cytoplasmic GTPase, the *Neu* oncogene (also called c-erbB-2 or Her2/neu in humans) encodes a tyrosine kinase receptor, which is amplified and overexpressed in as many as 30% of human breast cancers [24–27].

Using scintigraphic imaging, we demonstrated specific active TPT transport in adenocarcinomas in both mice (Fig. 4). Injected TPT accumulated in the stomach and tumor (Fig. 4*b*, MMTV–*Ras*, and *g*, MMTV–*Neu*). TPT accumulation was prevented when the isotope was co-injected with perchlorate (Fig. 4*c*, MMTV–*Ras*, and *h*, MMTV–*Neu*), showing that the accumulation in the tumor and stomach was specifically mediated by NIS. Injection of ^{99m}Tc-labeled human serum albumin (^{99m}Tc-HSA), a vascular space marker, proved that accumulation of TPT in the adenocarcinoma was not due to tumor blood pooling (Fig. 4*d*). Quantification of data shown for the *Ras* mouse (Fig. 4*e*) confirmed both the absence of TPT tumoral accumulation when co-injected with perchlorate and the lack of accumulation of ^{99m}Tc-HAS (Fig. 4*e*). We also demonstrated mgNIS expression by immunoblot analysis in both *Ras* (Fig. 4*f*) and *Neu* (Fig. 4*i*, lane tu1) tumors, showing that iodide transport results from mgNIS expression. Contralateral nontumoral mammary glands from the same MMTV–*Neu* mouse showed no mgNIS expression (Fig. 4*i*), indicating that the factors leading to the expression and activation of mgNIS in mammary gland tumors were not functional in *Neu* mouse nontumoral mammary glands. We found no TPT transport activity on imaging and no mgNIS expression on immunoblots in a second carcinoma in the same MMTV–*Neu* mouse (Fig. 4*i*, lane tu2). Immunohistochemically, there was no *Neu* expression in normal glands, whereas it was distinctly detectable in the adenocarcinoma that expressed mgNIS (Fig. 4*j* and *k*) and only minimally (about 5%) in the tumor that did not express mgNIS (data not shown). These observations indicate that tracer uptake in these tumors correlates with mgNIS expression in the same tumors. Although it is possible that radioiodide uptake in these adenocarcinomas was lower (on a per-cell basis) than in healthy lactating mammary gland, uptake was still sufficiently large to make it distinctly detectable by scintigraphy.

Expression of mgNIS in human breast cancer

We examined human breast tissue specimens for mgNIS expression, including 8 normal specimens from reductive mammoplasties, 29 malignant specimens (23 invasive carcinomas and 6 ductal carcinomas *in situ)*, 13 extratumoral specimens from tissue in the vicinity of the tumors, and 3 biopsies from pregnant women with breast nodules (Table 1). We studied the specimens by immunohistochemical analysis using two polyclonal antibodies (Ct-1 and Ct-2) and one monoclonal NIS-specific antibody (Fig. 5). We used antibodies against cytokeratin in parallel sections to distinguish breast epithelial cells from other stromal cell populations (data not shown). We rated sections by the intensity of the immunoperoxidase reaction on a scale of 0 to 4+, and considered samples to be positive for mgNIS expression if they had 2+ to 4+ staining in 20% or more of their epithelial cells.

We found that 87% of the 23 invasive carcinomas (Fig. 5*d*, *f* and *h*) and 83% of the 6 ductal carcinomas *in situ* (Fig. 5*i*) expressed mgNIS, compared with only 23% of the 13 noncancerous samples adjacent to or in the vicinity of the tumors (Fig. 5*g*). In addition, none of the eight normal samples from reductive mammoplasties expressed mgNIS (Fig. 5*b*). We detected both plasma membrane and intracellular staining in some malignant breast cells (Fig. 5*d*, *f*, *h* and *i*), in contrast to the distinct basolateral plasma membrane staining of rat lactating mammary gland tissues (Fig. 1*f*) and control salivary gland sections (Fig. 5*a*). Only 23% of extratumoral specimens showed staining (Fig. 5*g*), which was always less intense than that in malignant tissue (Fig. 5*d*, *f*, *h* and *i*). All three gestational biopsies showed characteristic adenomatous–lactational changes and were clearly mgNIS-positive (Fig. 5*c*). In conclusion, more than 80% of the breast cancer specimens analyzed expressed mgNIS, in contrast to no expression in normal tissues from reductive mammoplasties, indicating that mgNIS is upregulated with a high frequency during malignant transformation in human breast.

Discussion

Here we have reported the identification of the mgNIS protein and demonstrate that mgNIS catalyzes iodide accumulation in lactating mammary gland. mgNIS is present exclusively in the mammary gland during gestation and lactation (Fig. 2), in contrast to the constitutive expression of NIS in the thyroid (Fig. 1). Hormonal regulation experiments showed that a threshold level of circulating estrogens seemed to be necessary for optimal mgNIS expression overall, and in particular for the upregulation of mgNIS by oxytocin (Fig. 3). The cooperative function of estrogens in the effect of oxytocin on mgNIS may be explained by the likelihood that oxytocin receptor mRNA is upregulated by estrogen in the breast, as it is in the hypothalamus and uterus[28]. Additionally, estrogen may have a direct effect on mgNIS transcription, as the NIS promoter contains several half-site estrogen-responsive elements[29].

The antagonistic effect of prolactin on the oxytocin-induced increase of mgNIS expression may be due to the reported inhibitory effect of prolactin on steroidogenesis[30–33]. In intact, nongestational, nonlactating animals, exogenous prolactin would cause endogenous estrogen levels, which are lower than those in gestational or lactating animals, to decrease below the threshold, preventing concomitantly administered oxytocin from stimulating mgNIS expression. Conversely, in ovariectomized mice that received a high amount of exogenous estrogen, this antagonistic effect of prolactin co-administered with oxytocin did not occur; in fact, prolactin led to higher mgNIS expression (Fig. 3*e*, lane 8). This indicates that in the presence of high levels of estrogen, prolactin may have a separate direct or indirect stimulatory effect on mgNIS expression by an as yet unknown mechanism. The concentration of endogenous prolactin in intact animals, even during lactation, is considerably lower (about 1.2 μg/ml) than that used experimentally (300 μg/injection; ref. 34). Therefore, during lactation, estrogens would remain above the necessary threshold for oxytocin to stimulate mgNIS expression and for prolactin to enhance, rather than antagonize, this effect. Given the involvement of oxytocin in the increase of mgNIS expression, it is likely that the ability of progesterone to inhibit the combined stimulatory effect of 17-β-estradiol, oxytocin and prolactin on mgNIS expression may involve a direct inhibition of oxytocin receptor signaling by competitive binding of progesterone to the oxytocin receptor in the breast, similar to progesterone's effect in the uterus[28,35].

In vivo scintigraphic imaging of experimental mammary adenocarcinomas in nongestational and nonlactating female transgenic mice carrying either an activated *Ras* oncogene or overexpressing the *Neu* oncogene demonstrated pronounced, active, specific mgNIS activity that can be inhibited by perchlorate. Because these tumors are estrogen-receptor negative (data not shown), these observations indicate that mgNIS expression may also be induced by nonhormonal factors involved in the malignant transformation of mammary epithelial cells. The potential diagnostic value of the high prevalence of mgNIS expression (more than 80%) in human breast cancer (mgNIS was almost absent in normal tissue) becomes very apparent compared with the prevalence of the main current breast cancer marker Her2/*neu* (33%). Furthermore, that mgNIS-positive tumors from transgenic mice show active iodide transport indicates that radioiodide may be a possible alternative therapeutic modality in breast cancer.

The effectiveness of radioiodide therapy in treating thyroid cancer relies on the capacity of malignant thyroid cells to retain sufficient iodide transport activity to accumulate the isotope, even though this activity is relatively decreased as a result of malignant transformation compared with that of healthy thyroid cells. In contrast, the potential effectiveness of radioiodide therapy in breast cancer depends on whether mgNIS becomes functionally expressed in malignant mammary cells, given that it is only functionally expressed in healthy cells during pregnancy and lactation. It has generally been assumed, but has never been unequivocally proven, that iodide 'organification' (iodination of some tyrosyl residues of thyroglobulinz) occurs in thyroid cancer metastases. However, it is not clear that iodide organification in these metastases, even if it is present, actually increases the time of exposure of malignant cells to the radioisotope, considering the absence of follicular architecture[36]. More likely, the lack of an enclosed colloid compartment results in the release of organified iodide at a rate conceivably similar to that prevailing in the absence of iodide organification[37], whereas some thyroid metastases are devoid of iodide organification[38]. In addition, radioiodide therapy has been very successful in experimental prostate cancer *in vitro* and *in vivo* after tissue-specific expression of NIS (J.C. Morris, personal communication). Because there is no iodide organification in this system, this report indicates that radioiodide therapy can be effective in iodide-transporting, non-iodide-organifying tissues, a description that may apply to breast cancer tissue. Moreover, as thyroid NIS and mgNIS are regulated differently, it would be possible to protect the thyroid in the event of radioiodide administration to breast cancer patients. Thyroid suppression with exogenous T_3 leads to inhibition of TSH release and concomitant downregulation of thyroid NIS (ref. 3).

The most direct way to determine the activity of mgNIS in breast cancer is to subject patients to scintigraphic evaluation with TPT. A few preliminary reports using such an approach indicate that mgNIS is active in breast cancer[39]. However, when these studies were done, no specific uptake of the tracer in the tumors by NIS could have been expected or thoroughly analyzed. Therefore, the observed uptake was mistakenly considered 'nonspecific'. More recently, a patient undergoing neoadjuvant hormonal therapy for locally advanced breast cancer, who initially presented with an enlarged thyroid, underwent whole-body TPT scanning for thyroid evaluation. Definite evidence of tracer concentration in the area of the patient's breast invasive ductal carcinoma was found in the scintigraphic image. This meaningful (albeit preliminary) finding supports the idea that radioiodide therapy may be effective as an adjuvant to surgical treatment of primary breast cancer and/or systemic metastatic disease. An extensive separate study of scintigraphic TPT uptake in breast cancer patients may prove valuable and informative. The evidence presented here is an argument in favor of doing extensive studies to determine whether radioiodide may be an effective new option in the diagnosis and treatment of breast cancer.

Methods

Generation of site-directed antibodies. The following peptides corresponding to C-terminal sequences of the human NIS protein[40] were synthesized by solid phase synthesis[41] and used to generate polyclonal human NIS-specific antibodies Ct-1 and Ct-2, respectively: peptide P-857 (KELEGAGSWTPCVGHD) corresponds to residues 618–633, and peptide P-858 (GHDGGRDQQETNL) corresponds to residues 631–643. Polyclonal antibodies were generated and purified as described[3]. Peptide NEDLLFFLGQKELE, corresponding to residues 598–621, was used to generate the site-directed monoclonal antibody. Antibody against rat NIS protein[3] was used for immunological analysis of rodent tissues. Antibody against Her2/*neu* was purchased from DAKO (Carpenteria, California).

Nuclear imaging. Imaging was conducted using a scintigraphic gamma-camera system (Dyna Camera 4C; Picker International, Highland Heights, Ohio) with a pinhole collimator interfaced to a Macintosh computer-based nuclear medicine imaging system (NucLear MAC 3.01; Scientific Imaging, Littleton, Colorado). Appropriate energy peaks with 20% windows were used. Animals were anaesthetized with sodium pentobarbital. Technetium–pertechnetate (TPT ($^{99m}TcO_4^-$); Syncor International, Bronx, New York) was diluted in 0.9 N sodium chloride to a specific activity of 1.5 mCi in 0.2 ml volume, and injected into the tail vein before the mice were placed under the collimator. Human serum albumin was labeled with ^{99m}Tc by a modification of the protocol from a commercially available radiopharmaceutical kit (Technetium HSA Multidose; Amersham, Piscataway, New Jersey). Contents were dissolved in 0.5 ml sterile water and labeled by addition of 30 mCi TPT in a volume of 0.5 ml saline. After 20 min incubation, an 0.5-ml aliquot of the reaction mixture was placed on a size-exclusion column (Sephadex G-25 M column; Pharmacia Biotech, Piscataway, New Jersey) and eluted by stepwise addition of 0.5 ml PBS. Radiochemical purities of the initial kit product and purified peak fraction were 89% and 98.5%, respectively, as determined by instant thin-layer chromatography on ITLC-SG paper (Gelman Instrument, Ann Arbor, Michigan) using 85% methanol as solvent. ^{99m}Tc-HSA (1.5 mCi) was administered in a volume of 0.2 ml. Perchlorate was administered in 0.2 ml PBS at concentrations of 20 mg and 2 mg to rats and mice, respectively. Consecutive studies in previously lactating rats or transgenic mice were separated by 2 days (eight half-lives) to avoid interference between examinations.

Immunohistochemical analysis. Sections (5 μm) were deparaffinated and rehydrated. All slides were subjected to antigen retrieval using 10% citrate buffer (DAKO, Carpinteria, California). Samples were washed for 5 min in Tween-supplemented Tris-buffered soultion (0.3M sodium chloride, 0.1% Tween 20 and 0.05 M Tris-HCl, pH 7.6). Endogenous biotin activity was blocked with DAKO Biotin Blocking System (Carpenteria, California). The Catalyzed Signal Amplification kit (DAKO, Carpenteria, California) was used for the remainder of the procedure, according to supplier's instructions. Slides were incubated for 15 min with antibody against rat NIS, Ct-1 or Ct-2, or monoclonal primary antibodies. The initial concentrations of polyclonal and monoclonal antibodies were 1 μg/μl and 0.5 μg/μl, respectively. These were diluted in the provided blocking solution to a concentration of 1:500 (rat tissues), 1:600 (human salivary gland and breast, polyclonal antibodies), 1:750 (human thyroid, polyclonal antibodies) or 1:100 (human tissues, monoclonal antibody). Immunoreactivity was competitively inhibited in the presence of 0.7 μM corresponding synthetic peptides used to generate antibodies. Nonspecific immunoreactivity was evaluated with unrelated rabbit and mouse immunoglobulins (DAKO, Carpenteria, California). CAM 5.2 antibody against low-molecular-weight keratins 8 and 18 (Becton Dickinson, San Jose, California) was used to identify epithelial cells. All slides were counterstained with toluidine blue. Immunoreactivity was analyzed by light microscopy and graded on a scale of 0–4+. Tissues were judged positive for NIS expression when at least 20% or more of the cells had scores of 2+.

Hormonal treatment of animals. Either ovariectomized or intact CD1(ICR)IBR mice 8–10 weeks old (Charles River Laboratories, Wilmington, Massachusetts) were treated once a day with subcutaneous injections of 1 international units (IU) oxytocin (α-hypophamine), 10 IU prolactin, 1 μg 17-β-estradiol (1,3,5[10]-estratriene-3,17β-diol), or 1 IU progesterone (4-pregnene-3,20-dione) for 3 consecutive days, either individually or in the indicated combinations. All hormones were purchased from Sigma. Hormones were dissolved following the manufacturer's protocol and were injected in a volume of 200 μl sterile PBS, or, for progesterone (10 mg/ml), in 100 μl sesame oil. Control animals, which were sham-treated with sesame oil, were systematically included in experiments when progesterone was administered. A last injection was administered on the fourth day. Animals were killed 2 h later, followed by extirpation of mammary glands. At least three identically treated animals were analyzed in each case.

***In vivo* transport studies.** ^{125}I (1 μCi at 100 mCi/ml; Amersham-Pharmacia, Piscataway, New Jersey) was added to 100 μl PBS and intraperitonally administered to hormonally treated animals. Then, 1 h later, animals were killed and organs were placed in pre-weighted microfuge tubes. Approximately 500 μl blood was also obtained from the inferior vena cava of each animal. Tubes were weighted and counted in a γ-counter (LKB-Wallac, Gaithersburg, Maryland). Radioactivity accumulated in each organ was determined as counts per minute/mg tissue, standardized with radioactivity detected per mg blood, and expressed as the ratio of counts per minute detected in the organ of interest versus blood. Data were obtained from the analysis of at least three animals in each experiment.

Tissue retrieval and immunoblot analysis. Sprague-Dawley female rats (more than 8 weeks old) at different physiological stages, and hormonally-treated CD1(ICR)BR female mice were killed in a carbon dioxide chamber before excision of thoracic, abdominal and inguinal mammary glands. Organs removed from mice or rats were blended for 1 min with a polytron homogenizer (Brinkmann Instruments, Westbury, New York), and homogenized with a stirrer-type glass-Teflon homogenizer (Caframo-Wiarton, Ontario, Canada). Membrane fractions were prepared as described[42]. Samples were diluted 1:2 with loading buffer and heated at 37 °C for 30 min before being separated by SDS–PAGE, followed by electroblotting to nitrocellulose[3]. Immunoblot analyses used 40 μg membrane protein per lane, 0.2 μg/ml affinity-purified NIS-specific antibody[3] and horseradish-peroxidase-linked, rabbit-specific donkey IgG diluted 1:1,500 (Amersham-Pharmacia, Piscataway, New Jersey).

Peptidyl *N*-glycosidase F treatment. Membranes (40 μg) were resuspended in 10 μl 0.5 M Tris-HCl (pH 8.0), and 18 μl water was added with either 3 μl (600 milliunits) peptidyl *N*-glycosidase F (Boehringer Mannheim, Indianapolis, Indiana) or 2 μl 50% glycerol. Membranes were incubated overnight (18 h) at 37 °C, then diluted 1:2 with loading buffer (15 μl) and incubated at 37 °C for 30 min before electrophoresis[3].

Cyanogen bromide treatment. Pieces of nitrocellulose containing the corresponding immunoreactive NIS species were excised and cut into smaller pieces about 1 mm × 2 mm in size, and were incubated for 1 h in the dark at room temperature with 300 μl cyanogen bromide (about 300 mg/ml) in 70% formic acid. Samples were centrifuged to pellet nitrocellulose pieces; the formic acid containing the released digested peptides was lyophilized in a Speed-Vac at medium heat for about 1 h. Dried peptides were resuspended in 75 μl water and lyophilized again, followed by resuspension in 30 μl sample buffer. Samples were neutralized with a small volume (< 5 μl) of 100 mM Tris, pH 9.1, before being separated by 15% SDS–PAGE.

Acknowledgments

We thank A. De la Vieja and C. Riedel for computer assistance, G. Orr for advice and T. Ciao and G. Dai for help with animal experiments. We also thank L. M. Amzel, T. Graf, and the members of the Carrasco laboratory for reviewing the manuscript. O.L. was supported by the National Institutes of Health Hepatology Research Training Grant DK-07218. R.G.P. is a recipient of the Irma T. Hirschl award. This work was supported in part by R29CA70897 and RO1CA75503 (to R.G.P.). Work at the Albert Einstein College of Medicine was supported by Cancer Center Core National Institutes of Health grant 5-P30-CA13330-26. This project was also supported by the National Institutes of Health DK-41544, the Susan G. Komen Breast Cancer Foundation, the American Cancer Society BE-79422, and the Irma T. Hirschl award (N.C.).

RECEIVED 11 MAY; ACCEPTED 23 JUNE 2000

1. Carrasco, N. Iodide transport in the thyroid gland. *Biochim. Biophys. Acta* **1154**, 65–82 (1993).
2. Dai, G., Levy, O. & Carrasco, N. Cloning and characterization of the thyroid iodide transporter. *Nature* **379**, 458–460 (1996).
3. Levy, O. *et al.* Characterization of the thyroid Na^+/I^- symporter with an anti-COOH terminus antibody. *Proc. Natl. Acad. Sci. USA* **94**, 5568–5573 (1997).
4. Levy, O. *et al.* N-linked glycosylation of the thyroid Na^+/I^- Symporter (NIS): implications for its secondary structure model. *J. Biol. Chem.* **273**, 22657–22663 (1998).
5. Eskandari, S. *et al.* Thyroid Na^+/I^- symporter: mechanism, stoichiometry, and specificity. *J. Biol. Chem.* **272,** 27230–27238 (1997).
6. Stubbe, P., Schulte, F.J. & Heidenmann, P. Iodine deficiency and brain development. *Biblthca. Nutr. Dieta* **38**, 206–208 (1986).

7. Mountford, P.J., Coakley, A.J., Fleet, I.R., Hamon, M. & Heap, R.B. Transfer of radioiodide to milk and its inhibition. *Nature* **322**, 600 (1986).
8. DeGroot, L.J. in *Endocrinology* (ed. DeGroot, I.J.) 821–833 (Grune & Stratton Inc., Orlando, 1989).
9. *Werner & Ingbar's The Thyroid* 8th edn. (eds. Braverman, L.E. & Utiger, R.D.) 295–316 (Lippincott Williams & Wilkins, Philadelphia, 2000).
10. Nishizawa, K. *et al*. ^{131}I in milk and rain after Chernobyl. *Nature* **324**, 308 (1986).
11. Hill, C.R., Adam, I., Anderson, W., Ott, R.J. & Sowby, F.D. Iodine-131 in human thyroids in Britain following Chernobyl. *Nature* **321**, 655–656 (1986).
12. Balter, M. Chernobyl's cancer toll. *Science* **270**, 1758–1759 (1995).
13. Mazzaferri, E.L. NCCN thyroid carcinoma practice guidelines: NCCN proceedings. *Oncology* **13**, 391–442 (1999).
14. Greenlee, R.T., Murray,T., Bolden, S. & Wingo, P. Cancer statistics 2000. *A Cancer Journal for Clinicians* **50**, 7–33 (2000).
15. Socolow, E.L. & Ingbar, S.H. Metabolism of ^{99m}pertechnetate by the thyroid gland of the rat. *Endocrinology* **80**, 337–344 (1967).
16. Spitzweg, C., Joba, W., Eisenmenger, W. & Heufelder, A.E. Analysis of human sodium iodide symporter gene expression in extrathyroidal tissues and cloning of its complementary deoxyribonucleic acids from salivary gland, mammary gland, and gastric mucosa. *J. Clin. Endocrinol. Metab*. **83**, 1746–1751 (1998).
17. Wakerley, J.B., O'Neill, D.S. & ter Haar, M.B. Relationship between the suckling-induced release of oxytocin and prolactin in the urethane-anaesthetized lactating rat. *J. Endocrinol.* **76**, 493–500 (1978).
18. Higuschi, T., Honda, K., Fukuoka, T., Negoro, H. & Wakabayashi, K. Release of oxytocin during suckling and parturition in rat. *J. Endocrinol*. **105**, 339–346 (1985).
19. McCormack, J.T. & Greenwald, G.S. Progesterone and oestradiol-17-_ concentrations in the peripheral plasma during pregnancy in the mouse. *J. Endocrinol*. **62**, 101–107 (1974).
20. Rosenblatt, J. S., Mayer, A. D. & Giordano, A. L. Hormonal basis during pregnancy for the onset of maternal behaviour in the rat. *Psychoneuroendocrinol*. **13**, 29–46 (1988).
21. Sinn, E. *et al*. Co-expression of MMTV/*V-Ha-ras* and MMTV/c-*myc* genes in transgenic mice: synergistic actions of oncogenes *in vivo*. *Cell* **49**, 465–475 (1987).
22. Guy, C.T. *et al*. Expression of the *neu* protooncogene in the mammary epithelium of transgenic mice induces metastatic disease. *Proc. Natl. Acad. Sci. USA* **89**, 10578–10582 (1992).
23. Hung, M. & Lau, Y. Basic science of HER-2/*neu*: a review. *Semin. Oncol*. **26**, 51–59 (1999).
24. Slamon, D.J. *et al*. Human breast cancer: correlation of relapse and survival with amplification of the HER-2/*neu* oncogene. *Science* **235**, 177–182 (1987).
25. Paterson, M.C. *et al*. Correlation between c-erbB-2 amplification and risk of recurrent disease in node-negative breast cancer. *Cancer Res*. **51**, 556–567 (1991).
26. Siegel, P.M., Ryan, E.D., Cardiff, R. D. & Muller, W. J. Elevated expression of activated forms of neu/ErbB-2 and ErbB-3 are involved in the induction of mammary tumors in transgenic mice: implications for human breast cancer. *EMBO J*. **18**, 2149–2164 (1999).
27. DiGiovanna M.P. Clinical significance of HER-2/*neu* overexpression. *Principles and Practice of Oncology* **13**, 1–10 (1999).
28. Zingg, H.H. *et al*. in *Vasopressin and Oxytocin, Advances in Experimental Medicine and Biology* (eds. H.H. Zingg, Bourque, C.W. & Bichet, D.G.) 287–297 (Plenum, New York, 1998).
29. Ohno, M., Zannini, M., Levy, O., Carrasco, N. & DiLauro, R. The paired domain transcription factor Pax8 binds to the upstream enhancer of the rat sodium/iodide symporter gene and participates in both thyroid-specific and cAMP dependent transcription. *Mol. Cell. Biol*. **19**, 2051–2060 (1999).
30. Dorrington, J. & Gore-Langton, R.E. Prolactin inhibits oestrogen synthesis in the ovary. *Nature* **290**, 600–602 (1981).
31. Gitay-Goren, H., Lindenbaum, E.S. & Kraiem, Z. Prolactin inhibits hCG-stimulated steroidogenesis and cAMP accumulation, possibly by increasing phosphodiesterase activity, in rat granulosa cell cultures. *Mol. Cell. Endocrinol*. **61**, 69–76 (1989).
32. Krasnow, J.S., Hickey, G. J. & Richards, J.S. Regulation of aromatase mRNA and estradiol biosynthesis in rat ovarian granulosa and luteal cells by prolactin. *Mol. Endocrinol*. **4**, 13–21 (1990).
33. Villanueva, L.A., Mendez, I., Ampuero, S. & Larrea, F. The prolactin inhibition of follicle-stimulating hormone-induced aromatase activity in cultured rat granulosa cells is in part tyrosine kinase and protein kinase-C dependent. *Mol. Hum. Reprod*. **2**, 725–731 (1996).
34. Mattheij, J.A.M., Kuipers, M.A.G., Swarts, J.J.M. & Verstijnen, C.P.H.J. Intraperitonal infusion of EDTA in the rat blocks completely the prolactin rise in the plasma during suckling. *Horm. Res*. **16**, 219–229 (1982).
35. Grazzini, E., Guillon, G., Mouillac, B. & Zingg, H. H. Inhibition of oxytocin receptor function by direct binding of progesterone. *Nature* **392**, 509–512 (1998).
36. Fitzgerald, P.J. & Foote, F.W. Jr. The function of various types of thyroid carcinoma as revealed by the radioautographic demonstration of radioactive iodine. *J. Clin. Endocrinol*. **9**, 1153–1170 (1949).
37. Pochin, E.E., Cunningham, R.M. & Hilton, G. Quantitative measurements of radioiodine retention in thyroid carcinoma. *J. Clin. Endocrinol. Metab*. **14**, 1300–1308 (1954).
38. Valenta, L. Metastatic thyroid carcinoma in man concentrating iodide without organification. *J. Clin. Endocrinol*. **26**, 1317–1324 (1966).
39. Cancroft, E.T. & Goldsmith, S.J. ^{99m}Tc-pertechnetate scintigraphy as an aid in the diagnosis of breast masses. *Radiology* **106**, 441–444 (1973).
40. Smanik, P.A. *et al*. Cloning of the human sodium iodide symporter. *Bioch. Biophys. Res. Commun*. **226**, 339–345 (1996).
41. Carrasco, N., Herzlinger, D., Danho, W. & Kaback, H.R. Preparation of monoclonal antibodies against the lac permease of *Escherichia coli*. *Methods Enzymol*. **125**, 453–467 (1986).
42. Kaminsky, S.M., Levy, O., Salvador, C., Dai, G. & Carrasco, N. Na^+/I^- symport activity is present in membrane vesicles from thyrotropin-deprived non-I—transporting cultured thyroid cells. *Proc. Natl. Acad. Sci. USA* **91**, 3789–3793 (1994).